

Spatial Uniformity of Single Photon 1-D Imaging Detectors using Superconducting Tunnel Junctions

L. Li^a, L. Frunzio^a, C. M. Wilson^a, K. Segall^a, D. E. Prober^a,
A. E. Szymkowiak^b and S. H. Moseley^b

^a*Departments of Applied Physics and Physics, Yale University, CT 06520-8284*
^b*NASA Goddard Space Flight Center, MD 20771*

Abstract. We have developed single-photon, one-dimensional imaging detectors based on superconducting tunnel junctions. The devices have a Ta absorber with an Al/AlO_x/Al tunnel junction readout on each end. The best energy resolution is 13 eV FWHM at 6 keV in an area of 20 x 100 μm². For devices with a Nb ground contact to the center of the Ta absorber, the energy resolution is worse in the center of the Ta absorber. This nonuniformity is caused by the Nb ground contact. A device with a Ta ground contact to the base electrode of one of the junctions was tested. We obtain an energy resolution of 26 eV in the large region at the center of the absorber, where this energy resolution is determined by the junction response. The diffusion constant of Ta and the loss time of quasiparticles in Ta are also studied by measuring three devices with different size absorbers.

INTRODUCTION

Superconducting tunnel junction detectors (STJs) have been studied for use as single photon, non-dispersive spectrometers in a wide range of phonon energy, from 1eV to 10 keV [1-6]. The small superconducting energy gap, ~meV, compared to the electron-hole excitation energy, ~eV in semiconductors, gives a much larger (~10³) number of excitations, so the energy resolution of the STJ detectors is a factor of about $\sqrt{1000} \approx 30$ better than that of semiconductor detectors.

We are developing superconducting Nb-Ta-Al-AlO_x-Al tunnel junction detectors for astrophysical applications. The devices use a lateral double junction geometry which can implement 1-D spatial imaging with only 2 channel readouts. The devices studied have absorber lengths of 200 μm, 500 μm, or 1000 μm.

DEVICES AND EXPERIMENTAL SETUP

Three device geometries are shown in Fig. 1. Each has a superconducting Ta film ($\Delta_{\text{Ta}} = 0.7$ meV) 200 μm × 100 μm × 570 nm thick as the absorber. The calculated quantum efficiency is 28% at 6 keV. Devices A and B have a thin strip Nb contact

($\Delta_{\text{Nb}} = 1.5 \text{ meV}$) at the center. Device C has a Ta contact connecting to the base electrode of one of the junctions. The charge is read out by two Al-AlO_x-Al junctions, one on each end, which overlap the Ta by 10 μm . Devices A and C have junctions with area of 1680 μm^2 , and the area of each junction of device B is 510 μm^2 . When an x-ray photon is absorbed in the Ta, it breaks Cooper pairs and creates excess quasiparticles, which cool quickly to the gap edge. They then diffuse to each side, and after reaching one of the two Al regions (traps) they scatter inelastically toward the Al gap energy ($\Delta_{\text{Al}} = 0.18 \text{ meV}$) and become trapped in the Al. The quasiparticles then tunnel through the barrier and produce a current pulse. The integral of the current pulse gives the charge from each tunnel junction. The ratio of the charges collected at each junction determines the absorption location in one dimension, and the sum gives the energy of the x-ray photon. The two-junction geometry provides 1-D spatial imaging using the division of the quasiparticles between two junctions.

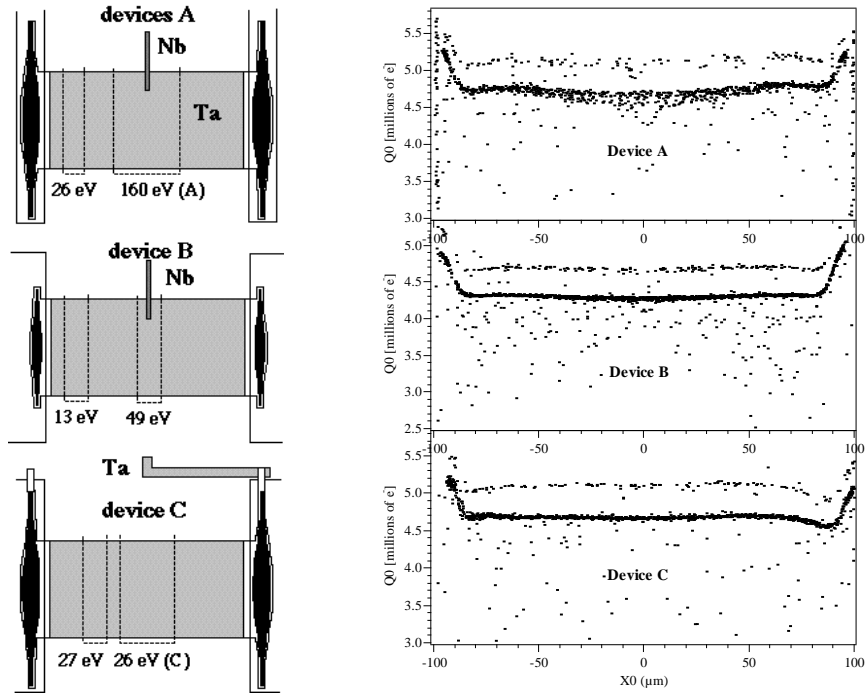


FIGURE 1. The geometries of the three devices and charge vs. location of the three devices after filtering and correction for the loss of the absorber and finite trapping. Black region is the junction; white region is the counterelectrode. Listed energies are the energy resolution for 5.9 keV photons for the location noted.

The devices are measured at a temperature of 210 mK. A magnetic field about 2.5 mT is applied parallel to the junctions to suppress the DC Josephson current, in order to voltage bias the junctions in the subgap region. The devices are illuminated with an ^{55}Fe x-ray source that emits $\text{MnK}_{\alpha 1}$ (5899 eV), $\text{MnK}_{\alpha 2}$ (5888 eV) and MnK_{β} (6490 eV) lines. The devices are biased and read out with a low noise current amplifier [7]. The detailed measurement results of the devices A [3,6,7] and B [8] have been published.

The signals are digitized and recorded by a Nicolet oscilloscope. Then the current signals are digitally filtered and integrated to get the charge.

EXPERIMENTAL RESULTS

Fig. 1 shows the total charge vs. absorption location of three devices after filtering and correction for absorber losses and finite trapping. The energy width (FWHM) is shown for various locations of each device. For devices A and B the energy resolution is degraded in the center of the absorber. But for device C, the energy resolution is uniform along nearly the whole absorber. The spatial nonuniformity in devices A and B is caused by the Nb contact. Niobium was used because its large energy gap should prevent quasiparticles from diffusing into the leads. However, Nb is also known to produce metallic suboxides, which may form local trapping sites on the Ta surface. Quasiparticles that are trapped at these regions could eventually recombine rather than tunnel. This would cause a dependence of the collected charge on distance from the Nb contact at the middle of the absorber. Absorption events which occur near the contact suffer more loss of charge than absorption events which occur away from the contact. This effect would give rise to data similar to Fig.1. For absorption events away from the center, we do not expect to see these effects. The 13 eV energy width for device B and the 26 eV width for device A appear to have no contribution from this effect, as known noise sources fully account for these widths [11]. Using a Ta contact to the Al base electrode instead can solve the nonuniformity problem caused by the Nb contact to the absorber. Fig. 1 shows that in the device with the Ta contact the broadening in the center is the same as away from the center. We obtain 26 eV energy resolution in a much larger area $50 \times 100 \mu\text{m}^2$ in the center.

Both devices A and C have energy resolution of 26 eV which is determined by the junction response. Their first Fiske mode occurs at 90 μV , limiting the bias voltage to 70 μV . The dominant noise sources of devices A and C result from incomplete cooling of the quasiparticles [9-10]. The reason that device B achieves 13 eV is that the junctions are smaller and the tunnel time (5 μs) is longer compared to devices A and C (2.5 μs). The quasiparticles cool longer before they tunnel, therefore the noise caused by bias voltage fluctuations and amplifier voltage noise are significantly reduced [9]. The Fiske mode of device B is at 150 μV , thus the junction can be biased at a higher voltage, which is also advantageous. The quantitative analysis of these effects will be presented elsewhere [11].

There is a small dip near the Ta contact side in the charge vs. location plot from device C. A possible explanation is that quasiparticles generated by an x-ray photon near that side of the device enter the Al before completely scattering down to the Ta gap. So, a small fraction of the quasiparticles can leak out the Ta ground contact before they are trapped in the Al. This broadens the energy resolution near that side to about 38 eV.

Device B shows some self-recombination effects due to the small trap volume. The ratio of the K_β to K_α line is 1.09 compared to the theoretical value of 1.10. For devices A and C the ratio is 1.10. Self-recombination is negligible in devices A and C, which have a larger trap volume. We expect that the use of a small junction with a Ta

ground contact to the Al base electrode will give a device with 13 eV resolution for most of the absorber. This design will need to increase the trap volume to reduce the self-recombination.

The physical properties of the Ta, such as the diffusion constant and quasiparticle loss time, are derived by measuring three devices with different lengths of absorbers (200 μm , 500 μm , 1000 μm) and the same size junctions and Nb contacts. These devices are like device A except for the absorber length. Simulations based on diffusion and tunneling models are used to fit the current pulse shapes and the delay time between the two pulses, in order to calculate the diffusion constant and quasiparticles loss time. The results are shown in Table 1. The fitting values for different devices are within 5%. The diffusion constant and the loss time determine the limit of count rate and size of the absorber of the STJ detectors. The 500 μm device shows some loss of quasiparticles in the center, but it can still give reasonable good energy resolution. The loss may be due to the Nb contact, and not the Ta absorber. If that is the case, a Ta ground contact must be used. This would allow the use of absorbers with dimension of $\sim 1\text{mm}$, as will be needed in some astronomy applications.

Absorber Size [μm^2]	Diffusion Constant [cm^2/s]	$(D \tau_{\text{loss}})^{1/2}$ [μm]	τ_{loss} of the qps [μs]
200 \times 100	8.0	263	87
500 \times 100	8.3	250	75
1000 \times 100	8.0	250	78
Average	8.1 \pm 0.2	254 \pm 5	80 \pm 5

Table 1. The diffusion constant and τ_{loss} of the quasiparticles for different sizes of Ta absorber.

ACKNOWLEDGMENTS

We thank R. Schoelkopf for useful discussions. This work was supported by NASA NAG5-5255.

REFERENCES

1. N. Booth and D.J. Goldie, Supercond. Sci. Technol. 9, 493 (1996).
2. H. Krauss, et al., Phys. Lett. B321, 195 (1989); J. Jochum, et al., Ann. Phys. 2, 611 (1993).
3. S. Friedrich, et al., Appl. Phys. Lett. 71, 3901 (1997).
4. P. Verhoeve, et al., Appl. Phys. Lett. 72, 3359 (1998); J.B. le Grand, et al., Appl. Phys. Lett. 73, 1295 (1998).
5. P. Hettl, et al., Proc. EDXRF'98, Bologna, 7-12 June 1998; G. Angloher, et al., Nucl. Instrum. Methods Phys. Res. A444, 214 (2000).
6. K. Segall, et al., IEEE Trans. Appl. Supercond. 9, 3226 (1999).
7. S. Friedrich, et al., IEEE Trans. Appl. Supercond. 7, 3383 (1997).
8. L. Li, et al., IEEE Trans. Appl. Supercond. 11, 685 (2001).
9. K. Segall, et al., Appl. Phys. Lett. 76, 3998 (2000).
10. K. Segall, Ph.D. Thesis, Yale University (1999), (unpublished).
11. L. Li, et al, submitted to J. Appl. Phys, (2001).